Wu *et al. Virology Journal* (2025) 22:246
https://doi.org/10.1186/s12985-025-02882-9

Virology Journal

RESEARCH Open Access

Quantum dot immunochromatographic strip for rapid and sensitive detection of H5 subtype avian influenza virus

Han Wu[1], Ping Wang[1], Jiamin Fu[1], Fan Yang[1], Linfang Cheng[1], Fumin Liu[1], Hangping Yao[1], Nanping Wu[1], Lihua Xu[2], Haibo Wu[1*] and Lanjuan Li[1*]

Abstract

The H5 subtype avian influenza viruses (AIVs) pose a major threat to wild fowl and poultry. Additionally, they can overcome the species barrier, inducing human infection, which may become fatal. Thus, the H5 subtype AIVs remain a global public health burden, with a huge pandemic potential. Therefore, it is imperative to establish a rapid, sensitive, and specific method for detecting H5 subtype AIV infection for diagnostic and preventive purposes. The quantum dot fluorescent microsphere-based immunochromatographic strip (QDFM-ICS) is being widely used for detecting various viruses. We here developed a pair of monoclonal antibodies (2F2 and 2B7) by immunizing mice with the A/duck/Zhejiang/6D2/2013(H5N6) virus and covalently linking them with quantum dots to generate a QDFM-ICS for detecting H5 subtype AIVs. The QDFM-ICS showed a limit of detection of 0.0625 hemagglutination units (HAU) per 80 µL for live H5 subtype AIVs and 1.2 ng/mL purified H5N6 hemagglutination protein, respectively. In addition, it demonstrated good reproducibility with a coefficient of variation of < 10%, showing a high degree of repeatability. The strips exhibited a full percentage of specificity. Notably, their sensitivity and specificity remained unaffected even when stored for 3 months at room temperature or 4 °C. Furthermore, the application in practical testing on field samples demonstrated a strong correlation between QDFM-ICS and real-time PCR. The QDFM-ICS can be used in less time, with a simpler operation, and lesser expenditure. Thus, QDFM-ICS is a practical and promising technique for detecting H5 subtype AIVs, especially in point-of-care testing.

Keywords Avian influenza virus, H5 subtype, Monoclonal antibodies, Quantum Dots, Fluorescent microsphere, Immunochromatographic strip

*Correspondence:
Haibo Wu
wuhaibo@zju.edu.cn
Lanjuan Li
ljli@zju.edu.cn
[1]State Key Laboratory for Diagnosis and Treatment of Infectious Diseases, and National Clinical Research Center for Infectious Diseases, the First Affiliated Hospital, School of Medicine, Zhejiang University, 79 Qingchun Road, Hangzhou 310003, Zhejiang, China
[2]Animal Husbandry and Veterinary Institute, Zhejiang Academy of Agricultural Science, Hangzhou 310021, China

Introduction

Avian influenza viruses (AIVs) belonging to the Orthomyxoviridae family, are negative-sense, single-stranded RNA viruses with eight gene segments containing haemagglutinin (HA), neuraminidase (NA), and six internal genes [1]. There are multiple subtypes of AIVs, which are classified based on the two glycoproteins, HA and NA. Since the past few decades, AIVs have become the most critical and virulent influenza virus that keep challenging both poultry and human health, posing substantial threats worldwide. Notably, the burden of AIVs is likely underestimated because of the limited diagnostic capabilities and inadequate surveillance of the animal–human interface [2]. Some AIV strains have resulted in distinct spillover events, such as H5, H7, H9, and H10, and can still trigger a future pandemic [3].The H5 subtype is a major circulating pathogen worldwide, raising great concern of potential pandemic threats via direct transmission from wild avian species to human beings [4].

The highly pathogenic avian influenza (HPAI) A virus strains (e.g., H5N1) were first reported from Hong Kong in 1996. They can be divided into 10 clades (clades 0–9) and various subclades [5, 6]. Clade 2.3.4.4 of AIV H5N1 is a strain that is still under circulation. This strain constantly reassorts with other NA genes, generating subtypes such as H5N1, H5N2, H5N3, H5N5, H5N6, and H5N8 [7, 8]. According to the World Animal Health Information System (OIE-WAHIS), HPAI has reportedly caused 9.1 million poultry infections and 93 outbreaks until December 2024 [9]. In addition, they have caused severe infections in humans as well. Since 2003 to 2025, the World Health Organization (WHO) has reported 964 cases of H5N1 infection in humans, with 466 fatalities (48%), across 24 countries [10]. Because of its wide distribution capability in birds, the virus has spread to Asia, North America, and Europe through bird migration. Since 2003, H5N1 has resulted in unprecedented pandemics in China and seven other east Asian countries, including Vietnam and Thailand, which reported several deaths too [11]. Since 2013, the H5N6 pandemic has been reported from Vietnam, Laos, and China with a high mortality rate among birds. This pandemic also infected at least 19 individuals in these countries, resulting in 13 fatalities [12, 13]. The reassortant clade 2.3.4.4 H5N8 HPAI virus is reportedly responsible for the poultry epidemic in South Korea in early 2014. This virus rapidly spread to Russia, Japan, and Europe [14, 15]. In late 2021, the Eurasian strain of H5N1 (clade 2.3.4.4b) was detected in North America, which led to an outbreak that continued until 2024 [4]. According to the US Centers for Disease Control and Prevention, clade 2.3.4.4b caused 15 human infections worldwide until October 2024 [16]. Apart from poultry and humans, these viruses can also break the species limitation barrier and cause infection spillover [17, 18], resulting in mammal-to-mammal transmission across various settings, such as US dairy cattle farms, marine mammals in South America, and European fur farms [19], adversely affecting public and animal health with heavy socioeconomic tolls.

Quantum dots (QDs) are nanoparticles of size between 1 and 10 nm. Because of their small size, they exhibit a quantum confinement effect. As a result, they have a high fluorescence efficiency and can resist photo bleaching. They also have other properties, such as wide excitation wave lengths, narrow, symmetric emission spectra, ultrahigh sensitivity, and excellent stability [20]. Therefore, they are widely used for fluorescent biological labeling, single-particle tracking, in vivo imaging [21], and virus detection, including the detection of major communicable viruses such as influenza A virus [22], SARS-CoV-2 [23], human immune deficiency virus [24], and Zika virus [25]. The commonly used test methods for these viruses, including enzyme-linked immunoassays assay (ELISA) [26] and real-time reverse transcriptase PCR (RT-PCR) [27], require specialized equipment and operators. In contrast, QDs are a rapid, sensitive, and portable detection technology for the isolation and identification of viruses. They can be employed for point-of-care testing (POCT) detection, which may help in rapid and efficient detection of H5 subtype AIVs, thereby helping with the surveillance and prevention of the infection. QDs can be used as a novel approach for improving immunoassay techniques [28]. Directly labeled QDs and conjugated QDs are already being used for bacterial detection. Compared to the traditional dyeing method, the QD method has a brighter fluorescence intensity, lower detection threshold, and improved accuracy in the analysis of bacterial cell mixtures [29]. Ongoing advances in the QDFM-ICS technology have revealed new avenues for sensitive, reliable, and economical detection and analysis of AIVs.

This study aims to develop and investigate two monoclonal antibodies (2B7 and 2F2) by immunizing mice with the H5 strain antigen protein and to design a QDFM-ICS method for determining the H5 subtype influenza antigen. We illustrated that the limit of detection (LOD) of the QDFM-ICS method for the hemagglutinin titer of the H5 subtype AIV was 2^{-4} per 80 μL of the sample and 1.2 ng/mL purified H5N6 HA protein, while its specificity could reach 100%, exhibiting the unique and exclusive combination characteristics of mAb 2F2 with the H5 subtype AIV. Its application in practical testing on field samples demonstrated a strong correlation between QDFM-ICS and real-time PCR. Along with qualified reproducibility and simplified procedures and instruments, QDFM-ICS could be used for swift and sensitive detection of H5 AIVs, especially under severe circumstances, such as potential highly pathogenic H5 AIV outbreaks.

Materials and methods

Cell lines, proteins, and viruses

The MDCK cell lines and SP2/0 mouse myeloma cells were cultured and maintained in our laboratory. Both were well cultured in complete DMEM (Gibco), comprising 10% FBS (Gibco) and 1% penicillin–streptomycin (Gibco), at 37 °C in a 5% (v/v) CO_2 atmosphere. The Avian Influenza Virus (H5 Subtype) Hemagglutination Inhibitor Test Antigen (H5-Re-8, Re-11, Re-13, and Re-14 strains) was obtained from Harbin Guosheng Biotechnology Co. Ltd (China). The H5 virus A/duck/Zhejiang/6D2/2013(H5N6) was previously isolated from poultry in eastern China by our laboratory [30]. All the cells and AIVs were stored at -80 °C. The viruses were propagated in 9-day-old specific pathogen-free (SPF) embryonated chicken eggs. The titers were determined using a TCID50 assay, as previously described, with hemagglutinin (HA) from 1% chicken red blood cells (RBCs) [31]. The H5 subtype AIVs were operated in an accredited Biosafety Level 3 (BSL-3) containment laboratory at the First Affiliated Hospital of Zhejiang University, China. All the viruses included are listed in Table 1.

Generation and characterization of murine monoclonal antibodies

All six-week-old, female, BALB/c mice were provided by SLAC Laboratory Animal Co. Ltd (China). These mice were well-bred in an SPF environment with 60% humidity and a constant temperature. Firstly, the H5N6 virus (A/duck/Zhejiang/6D2/2013) was mixed with the Quick Antibody mouse adjuvant (Biodragon) to immunize the BALB/c mice twice through intramuscular injection 2 weeks apart. Seven days after the last injection, the antibody concentrations were measured through indirect ELISA using the venous blood samples obtained from the mouse tail. The mouse with the highest antibody titer intraperitoneally received an additional single H5 antigen immunization boost. After 3 days, the splenocytes obtained from this mouse were fused with SP2/0 cells [32]. Subsequently, the hybridoma culture supernatants were screened through ELISA using HA-coated plates. Positive hybridoma cell lines were singled outby using the limiting dilution method for further culture. These hybridoma cells were then extensively expanded and harvested to produce ascites in pristane-stimulated BALB/c mice [31]. To obtain mAbs, the ascites was purified by using a Protein-G column (GE Healthcare), following the manufacturer's instructions. The concentrations of the purified mAbs were measured with NanoDrop™ 2000 (Thermo Fisher Scientific) and stored at − 80 °C for long-term usage. The type and subclass of the mAbs were confirmed by using a mouse mAb isotyping kit (Bio-Rad), as per the manufacturers' instructions. The light and heavy chains of these mAbs were sequenced by SinoBiological (Beijing, China) [31].

ELISA

On the first day, 96-well plates were coated by purified proteins (20 ng/well) and maintained overnight at 4 °C. On the second day, the plates were washed five times with phosphate-buffered saline (PBS) and were blocked using a blocking buffer (KPL, Milford, MA, USA) for the next 2 h. They were again washed five times, after which the supernatants of the selected hybridomas were added to each well (100 µL/well) and incubated for 2 h at room temperature. Horseradish peroxidase (HRP)-conjugated goat anti-mouse IgG (Novus) was used as the secondary antibody for another hour. Later, the absorbance of the substrate reactions was measured at 450 nm using a plate reader (Bio-Rad). The affinities of the mAbs were assessed using ELISA, as mentioned earlier [31]. Briefly, the purified mAbs were double-diluted to 10 µg/mL and then quantified using ELISA, as outlined above.

Immunofluorescence assay (IFA)

The sensitivity and specificity of various AIV subtypes (H5N1, H5N2, H5N6, and H5N8) and mAbs 2F2 and 1B7 were analyzed using IFA [33]. Firstly, pre-prepared MDCK cells were employed to achieve nearly 70% confluence of the well before infection and were administered with the virus at a multiplicity of infection (MOI) of 0.5. Following a 24-h incubation, the cells were washed with PBS and then fixed in 4% paraformaldehyde for 30 min at 25 °C. Next, the MDCK cells were treated with 0.5% Triton X-100 for 30 min at room temperature for permeabilization. Once these fixation steps were completed, the cells were washed three times with PBS. In addition, 3% bovine serum albumin (BSA) solution was used to block the cells for 1 h at room temperature. The solution was then discarded, and the cells were incubated overnight at 4 °C with mAbs 2F2 and 2B7 (10 µg/mL each). Isotype antibodies (IgG1 or IgG2a) were used as negative controls. The cells were again rinsed three times with PBS and were administered with the secondary antibodies (5 µg/mL) for another 90 min at 37 °C in the dark, followed by another three washes with PBS. Subsequently, the cells were incubated with goat anti-mouse IgG (H + L) and conjugated with Alexa Fluor 488 (Abcam, UK). The images were captured and analyzed using a Leica SP8 confocal laser scanning microscope (Leica, Germany).

Hemagglutination Inhibition (HAI) assay

The HAI was conducted as described in previous studies [34]. The HAI titer is the reciprocal of the highest dilution of an antibody sample that can completely inhibit RBC hemagglutination. The AIV solutions were diluted with 1% chicken RBCs and titrated by utilizing a

Table 1 The viruses included in this study

No	Virus	Strain name
1	H5N1 (2.3.2)	A/duck/Zhejiang/224/2011
2	H5N1(2.3.2)	A/goose/Zhejiang/727,098/2014
3	H5N1(2.3.4.4 g, Re 8)	A/chicken/Guizhou/4/13
4	H5N1(2.3.4.4b)	A/Texas/37/2024
5	H5N2 (2.3.4.4c)	A/chicken/Zhejiang/514,135/2015
6	H5N2 (2.3.4.4b)	A/duck/Zhejiang/6DK19/2013
7	H5N6 (2.3.4.4 h, Re 11)	A/duck/Guizhou/S4184/2017
8	H5N6 (2.3.4.4b)	A/duck/Zhejiang/6D2/2013
9	H5N6 (2.3.4.4b)	A/chicken/Zhejiang/528,127/2016
10	H5N6 (2.3.4.4 h, Re 13)	A/duck/Fujian/S1424/2020
11	H5N8 (2.3.4.4b)	A/duck/Zhejiang/W24/2013
12	H5N8(2.3.4.4b)	A/duck/Zhejiang/925,019/2014
13	H5N8 (2.3.4.4b, Re 14)	A/whooper swan/Shanxi/4 – 1/2020
14	H1N1 (pdm09)	A/California/07/2009
15	H1N2	A/duck/Zhejiang/D1/2013
16	H1N9	A/chicken/Zhejiang/51,043/2015
17	H2N8	A/duck/Zhejiang/6D10/2013
18	H3N2	A/duck/Zhejiang/4613/2013
19	H3N6	A/duck/Zhejiang/D1–3/2013
20	H4N2	A/duck/Zhejiang/727,145/2014
21	H4N6	A/duck/Zhejiang/409/2013
22	H6N1	A/chicken/Zhejiang/1664/2017
23	H6N2	A/duck/Zhejiang/727,038/2014
24	H6N6	A/chicken/Zhejiang/727,018/2014
25	H7N3	A/duck/Zhejiang/11/2011
26	H7N7	A/chicken/Jiangxi/C25/2014
27	H7N9	A/chicken/Zhejiang/DTID-ZJU01/2013
28	H7N9	A/Guangdong/HP001/2017
29	H9N2	A/chicken/Zhejiang/329/2011
30	H10N2	A/duck/Zhejiang/6D20/2013
31	H10N7	A/chicken/Zhejiang/2CP8/2014
32	H10N8	A/chicken/Zhejiang/102,615/2016
33	H11N3	A/duck/Zhejiang/727D2/2013
34	H11N9	A/duck/Zhejiang/71,750/2013
35	Newcastle disease virus	La Sota
36	Newcastle disease virus	Clone 30
37	Infectious bronchitis virus	H120
38	Infectious bronchitis virus	H52
39	Infectious bursal disease virus	NF8
40	Infectious bursal disease virus	B87
41	Avian paramyxovirus-4	ZJ-1
42	Marek's disease virus	FC-126
43	Infectious laryngotracheitis virus	K317
44	Avian Pox virus	Quail-Adapted strain

The vaccine strain H5-Re8 contains surface genes from a clade 2.3.4.4gvirus, A/chicken/Guizhou/4/13(H5N1) (GZ/4/13), and six internal genes from the high-growth A/Puerto Rico/8/1934 (H1N1) (PR8) virus, and the H5-Re11 strain that harbor surface genes from a clade 2.3.4.4 h virus, A/duck/Guizhou/S4184/2017(H5N6) (GZ/S4184/17), and internal genes from PR8. H5-Re13 contains the HA and NA genes from A/duck/Fujian/S1424/2020 (H5N6) and was developed to protect against H5 viruses carrying the clade 2.3.4.4 h HA gene and H5-Re14 contains the HA and NA genes of A/whooper swan/Shanxi/4 – 1/2020 and was developed to protect against H5 viruses carrying the clade 2.3.2.1b HA gene

concentration of eight HAU/25 μL. Positive and negative controls comprising the encompassed sera were sourced from immunized and normal mice, respectively. Next, we completed twofold successive dilutions of mAbs in 96-well microtiter plates with 25 μL of PBS/well. Next, an equal amount of the H5 virus was introduced to each well. We then performed a 30 min incubation at ambient temperature so that the mAbs and virus could

interact with each other. HAI was titrated with 50 µL of 1% chicken RBCs after 20 min of the incubation.

Virus microneutralization (MN) assay

The MN assay was performed following a previously described procedure [35]. The purified H5 mAbs (100 µg/mL) were serially diluted in 2-fold increments and then incubated with an equivalent volume of 100 TCID50 (50% tissue culture infectious doses) of the A/duck/Zhejiang/6D2/2013 (H5N6) virus at 37 °C for 2 h. Following PBS washing, the MDCK cells were infected with the mixtures and co-incubated for 1 h at 37 °C. Subsequently, *N*-tosyl-L-phenylalanine chloromethyl ketone (TPCK)-treated trypsin (Worthington) was supplemented to every well (Sect. 2.5) and incubated for 72 h at 37 °C. The cytopathic effect (CPE) was observed. The mAb titers necessary to inhibit virus replication by 50% (IC_{50}) were determined through HA assay, following the Reed and Muench method.

Generation of antibody escape mutants

The escape mutants were characterized so that the generated mAbs could recognize the conformational epitopes. First, each mAb was diluted to two concentrations (2 and 4 ng/mL) and mixed with 100 TCID50 of A/duck/Zhejiang/6D2/2013 (H5N6) virus for 1 h at 37 °C prior to inoculation into 9-day-old embryonated chicken eggs for 72 h at 35 °C. After harvesting and detecting the allantoic fluid using HA assay, we collected the positive allantoic fluid samples, which were again passed through the 9-day-old embryonated chicken eggs under the same control conditions, with 8 and 16ng/mL of mAb concentrations. The RNA was isolated using the Trizol LS reagent (Life Technologies). The HA segment was amplified using RT-PCR and the changes in the amino acid were detected by sequencing, as described in a previous study [31].

Development of QDFM-ICS method

The detection was performed based on the following principles [36]. As shown in Fig. 1, the H5 subtype of the influenza A virus or its purified proteins were conjugated with the QD-labeled antibodies and used as the detection line. The excrescent and unbound QD-labeled antibodies were bound to the goat anti-mouse IgG antibodies and employed as the reference line. An obvious fluorescent response was visible to the naked eye upon excitation by 365-nm ultraviolet radiations. The captured QDs could also be viewed by using a fluorescence test strip scanner.

Firstly, we dissolved 40 µL of QDs in 400 µL of 25-mM 4-morpholineethanesulfonic acid (MES, Sigma-Aldrich). These QDs were excited for 30 min using 15 µL of 1-ethyl-3- (3-dimethylaminopropyl) carbodiimide hydrochloride (EDC, Thermo Fisher Scientific) and *N*-hydroxysuccinimide (NHS, Sigma-Aldrich), each at a concentration of 10 mg/mL [37]. After removing the residual EDC and NHS, 0.2 mg of mAb 2F2 was added to the mixture to resuspend the QDs [23] and then treated with 400 µL of 2% BSA (Sangon Biotechnology) containing a buffer (such as BSA) for 1 h to block any non-specific binding. After wiping off the unbound antibodies and chemicals [38], the QD-mAb conjugations were resuspended in 180 µL of MES and applied onto glass cellulose membranes (Jiening Biotechnology). Next, 1 mg/mL of goat anti-mouse IgG (Solarbio) with 4 mg/mL of mAb 2B7 was applied to the nitrocellulose (NC) membrane (Sartorius) on a BioDotXYZ platform (Jinbiao Biotechnology) at a rate of 2 µL/cm to form a control and a test line. The treated NC membranes, absorbent pad, and sample pad were assembled together on a polyvinyl chloride (PVC) backplate, cut into 3.5-mm-wide strips by using an automatic cutting machine, and stored at 4 °C for subsequent use. The fluorescence could be viewed under 365-nm UV light by naked eyes and measured by using a fluorescence test strip scanner (Hemai Technology, China).

Specificity, sensitivity, repeatability, and stability of the H5 QDFM-ICS

We verified the specificity of H5 QDFM-ICS using various subtypes of AIVs (H5N1, H5N2, H5N6, H5N8, H1N1, H1N2, H2N8, H3N2, H3N6, H4N2, H4N6, H6N1, H6N2, H6N6, H7N3, H7N7, H7N9, H9N2, H10N2, H10N7, H10N8, H11N3, and H11N9) and other avian viruses such as Avian paramyxovirus-4 (APMV-4, ZJ-1), Infectious bronchitis virus (IBV, H120, and H52), Infectious bursal disease virus (IBDV, B87, and NF8), Marek's disease virus (MDV, FC-126), Infectious laryngotracheitis vírus (ILTV, K317), Avian pox virus (APV, quail-adapted strain), and Newcastle diseasevirus (NDV, Clone 30, and La Sota). Twice-diluted allantoic fluid containing 2^4–2^{-8} HAU of the H5N6 virus A/duck/Zhejiang/6D2/2013 (H5N6) and 1250 – 0.3 ng/ml of purified H5 HA protein was employed to test the sensitivity of the QDFM–ICS. Finally, we conducted a repetitive experiment as follows. The strips were added to 80 µL of the aforementioned H5N6 AIV allantoic fluid 20 times for each titer (2^4, 2^3, 2^2, 2^1, 2^0, 2^{-1}, 2^{-2}, 2^{-3}, and 2^{-4} HAU) to determine the coefficient of variation (CV) and the absorbance value. To evaluate the stability, the QDFM-ICS strips were randomly stored at 4°C, room temperature, and 40 °C separately for 1, 2, and 3 months, respectively, to test their detection performance (negative and positive) [39].

Assessment of H5 QDFM-ICS in vitro samples

To determine the actual efficacy of the QDFM-ICS technique, 160 field samples (30 throat swab, 30 cloacal swab, and 100 fecal samples) from ducks, chickens, and geese

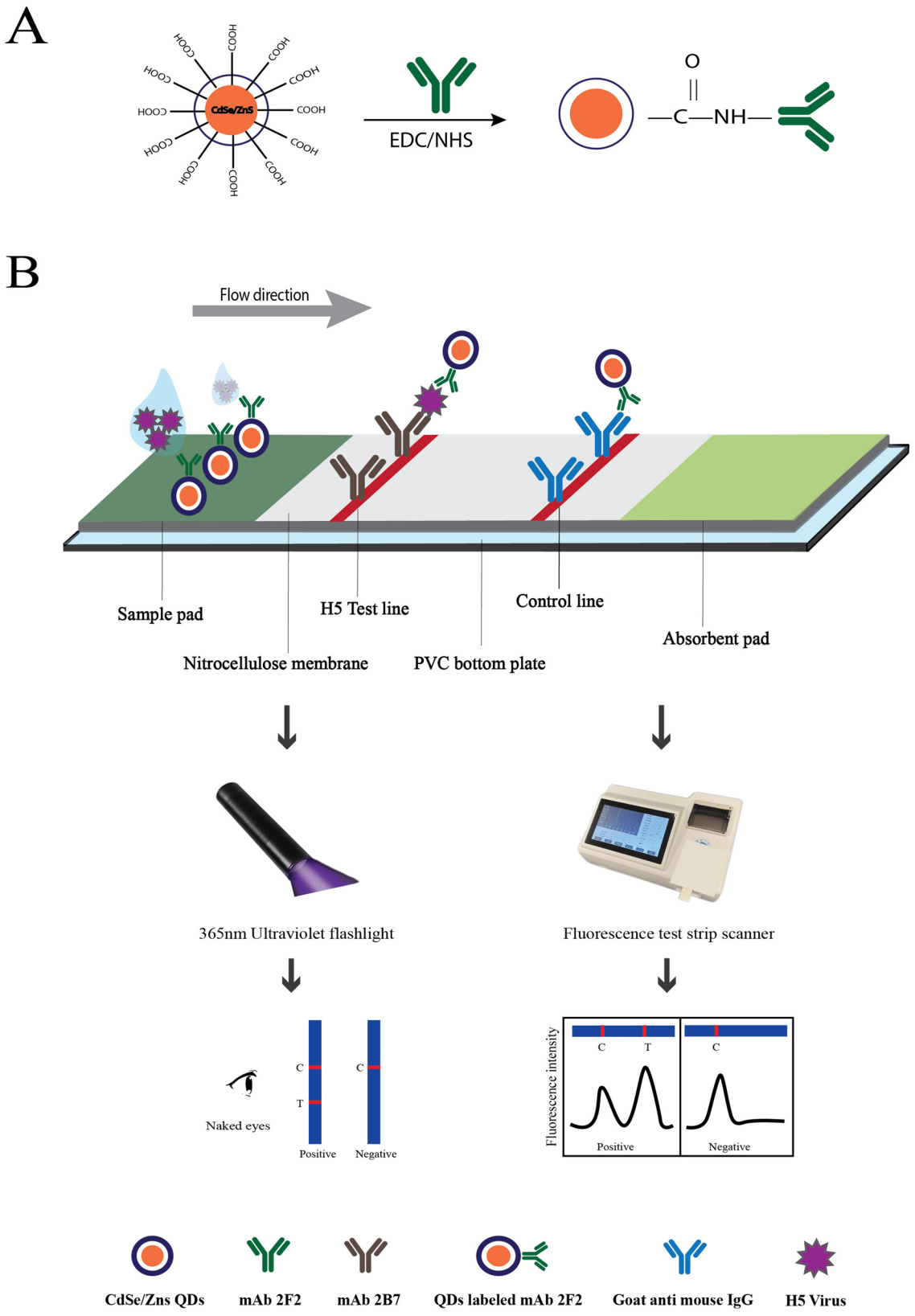

Fig. 1 Schematic demonstration of QDFM-ICS methods for the detection of AIV subtype H5. (**A**) EDC and NHS were used to activate the QDs. (**B**) Once the samples containing the target viruses flowed through the nitrocellulose membrane, the virus could be captured by the test line coated with mAb. The fluorescent band could be detected by 365-nm ultraviolet flashlight by naked eyes or scanned by using a fluorescence scanner

were collected and analyzed using real-time RT-PCR and QDFM-ICS. We considered the RT-PCR results as the control method. The data obtained were analyzed using the CFX96 System (Bio-Rad, CA, USA). All the samples were first dissolved in PBS and centrifuged. They were then kept first at room temperature for 1 h and then stored at -80 °C for long-term usage. Subsequently, A/Texas/37/2024 (H5N1), A/duck/Zhejiang/6DK19/2013 (H5N2), A/duck/Zhejiang/6D2/2013 (H5N6), and A/duck/Zhejiang/W24/2013 (H5N8) AIVs were added to the above samples to prepare spiked samples, 35 of which were confirmed as positive, for testing.

Results

Characterization of mouse anti-AIV H5 mAbs and QD–mAb conjugate

We produced two murine mAbs (2F2 and 2B7) using the hybridoma technology described previously [31]. Their isotype identification results are listed in Table 2. Both 2F2 and 2B7 mAbs belong to the IgG2a subclass. The sequences of their heavy- and light-chain regions are also presented in Table 2. An ELISA assessment showed that these two mAbs display a strong binding affinity to the HA protein of A/duck/Zhejiang/6D2/2013 (H5N6). In addition, the HAI assay showed that these mAbs inhibited the interaction between A/duck/Zhejiang/6D2/2013 (H5N6) and erythrocytes. This inhibitory effect could be achieved with up to 16 HAU/mL (Table 2). Besides, the MN assay demonstrated that both the mAbs can neutralize A/duck/Zhejiang/6D2/2013(H5N6) to 0.78ng/mL (Table 2). The IFA was conducted to verify the binding capacity of the mAbs with the H5 virus-infected MDCK cells. The detective indicator was assessed under fluorescence microscopy. As shown in Fig. 2, the IFA results indicated that the mAbs can specifically bind to the A/duck/Zhejiang/6D2/2013 (H5N6) and other H5 viruses, including A/goose/Zhejiang/727,098/2014 (H5N1), A/duck/Zhejiang/6DK19/2013 (H5N2), and A/duck/Zhejiang/W24/2013 (H5N8). However, they did not bind to other subtype influenza viruses (H1N2, H2N8, H3N2, H4N6, H6N1, H7N9, H9N2, H10N2, and H11N3 AIVs).

Phylogenetic and antigenic site analyses by selecting monoclonal antibody resistant mutants (MARMs)

Under the immunity pressure of the mAbs, we screened out the corresponding mutated epitopes by co-culturing the H5N6 virus A/duck/Zhejiang/6D2/2013 (H5N6) twice with different concentrations of target mAbs. Next, we collected the positive allantoic fluid samples containing the live virus to sequence and analyze the nucleotide sequence of their HA genes (Fig. 3). The mAb 2F2 escape virus had a single R239S mutation in its receptor-binding domain (RBD), while mAb 2B7 treatment contributed to A172T mutation at potential glycosylation sites. The 35,284 complete HA genes belonging to H5 were obtained from the GISAID and aligned by using the MEGA11 software. The conservation analysis of H5 HA residues substituted in mAb-resistant mutants revealed that R239S and A172T sites are conserved in the H5 AIV epidemic strains (Table 3). A total of 33,863 H5 HA gene sequences, acquired from the GISAID up to January 29, 2025, were aligned and analyzed by BioEdit. The percentages represent the proportion of amino acid mutation sites at positions 239 and 172 in the H5 AIV strains. The total occurrence probability of R239S and A172T mutations exhibited high conservation, exceeding 80%. However, the 172 epitope sites maintained their approximate mutation rates between alanine (A) and threonine (T) before 2005. This discovery was also applicable to the arginine (R) to serine (S) transformation at the 239 site. Apparently, both the epitopes demonstrated consistently high conservation of over 90% after 2020. This result suggested that the selected mutants, under the influence of mAbs 2B7 and 2F2, reverted to a more conserved state in the epidemic strains of recent years. Next, we visually presented the results of escape mutation sites, using the protein structure of the H5N6 virus A/duck/Zhejiang/6D2/2013 (H5N6) downloaded from the Protein Data Bank (PDB), to display the antigenic sites of the HA protein with different colors.

LOD of H5 QD-ICS

We used PBS to serially dilute H5 antigen HAI titers from 2^4 to 2^{-8} HAU or purified H5N6 HA protein from 1250 to 0.3 ng/mL to assess the LOD of the QD-ICS for

Table 2 Characterization of monoclonal antibodies (mAbs) 2B7 and 2F2

Clone	Isotype	Characteristics			Heavy chain		Light chain	
		Affinity (μg/ml)	HI titer (ug/ml)	MN titer (mg/ml)	V-GENE and allele	CDR3	V-GENE and allele	CDR3
2B7	IgG2a, κ	9×10^{-5}	>0.78	≥1	Musmus IGHV1-18*01 F	ARSDDHDAWFAY	Musmus IGKV1-135*01 F	WQGTHFPQT
2F2	IgG2a, κ	6×10^{-6}	>0.78	≥7	Musmus IGHV2-6-7*01 F	ARDGGYGYGFAY	Musmus IGKV12-46*01 F	QHFWGTPLT

The isotype of the mAbs was measured through the mouse mAb isotyping kit

The affinity, HI titer and MN titer reflected the properties of the mAbs through reaction with H5 virus A/duck/Zhejiang/6D2/2013 (H5N6) as mentioned before

V-gene refers to the variable region encoded by the DNA sequence

CDR3 refers to Complementarity-determining region

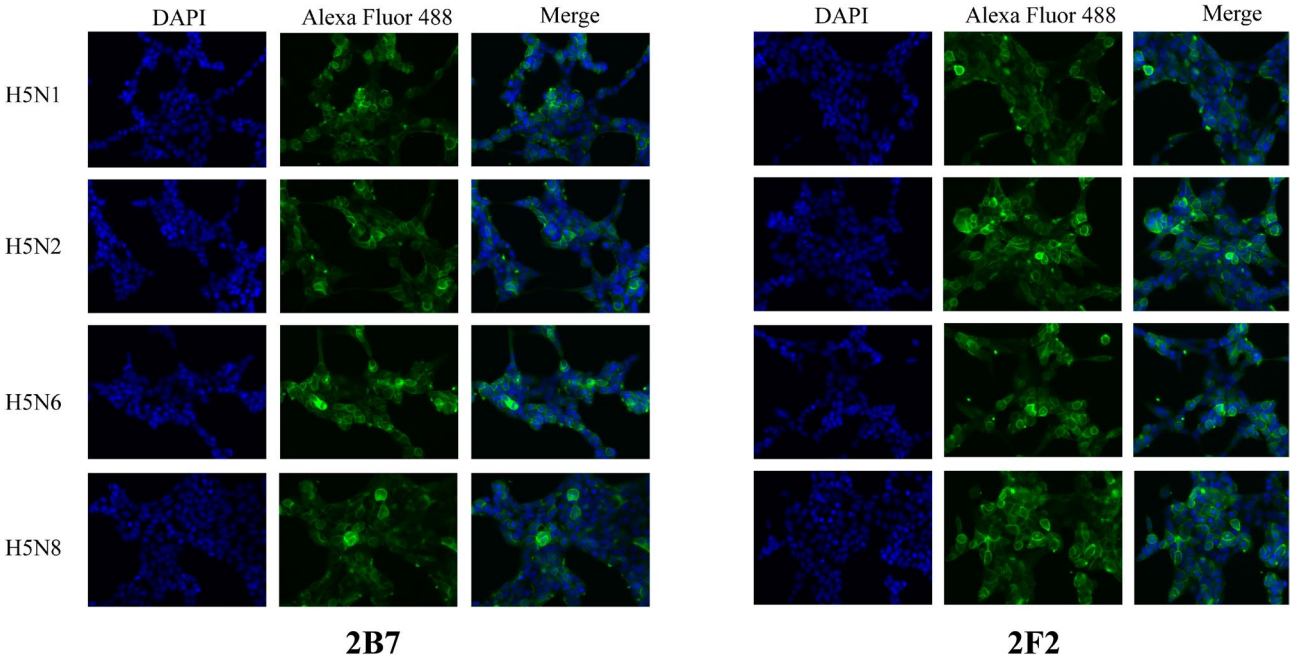

Fig. 2 Specificity of mAbs binding to different subtypes of influenza virus. IFA was conducted to measure the binding of mAbs to various influenza virus strains. The MDCK cells were infected with H5N1, H5N2, H5N6, and H5N8 influenza viruses at an MOI of 0.5. After subsequent fixation, permeabilization, and blocking, mAbs 2F2 and 2B7 were added to the incubation mixture. The binding of mAbs was detected by Alexa Fluor 488 (green) conjugated secondary antibodies. Then, the cells were stained with DAPI (blue), and fluorescent signals were observed by fluorescence microscopy. Note that mAbs 2B7 and 2F2 could combine with the H5 subtype of AIVs. Green, viral proteins; blue, nuclei

detecting H5 AIVs. Every dilution was given three replicate samples each. After adding the prepared samples for 15 min, the signals were observed under 365-nm ultraviolet excitation by naked eyes as well as through a fluorescence test strip scanner. Direct correlations were observed between the H5 antigen concentration and the fluorescence intensity of the test line. The fluorescence from the H5 antigen test line at 2^{-4} HAU (Fig. 4A) and 1.2 ng/mL purified H5N6 HA protein (Fig. 4B).

To assess non-specific adsorption, 20-mM PBS was applied to the nitrocellulose membrane, which was then used as the test line. Next, 1 mg/mL of goat anti-mouse IgG was applied to the strips and used as the control line. These strips and the nitrocellulose membrane were used to test H5 antigens at various concentrations. Very low fluorescence intensity was detected at the test line, indicating that the variation in fluorescence intensity can be attributed to the interaction between the immobilized antibodies and the virus.

Repeatability of H5 QDFM-ICS

The repeatability of the QDFM-ICS was evaluated by measuring absorbance from 20 replicates at different titers of the H5 virus, ranging from 2^4 to 2^{-4} HAU with serial 2-fold dilutions above the LOD value. The signals generated by 20 replicates at varying concentrations of the H5 virus were detected to test the reproducibility of this QDFM-ICS. As demonstrated in Table 4, all the CV values are below 10%, which indicates that the QDFM-ICS exhibits a high degree of repeatability.

Specificity of H5 QD-ICS

We examined other influenza virus subtypes (including H1N2, H2N8, H3N2, H4N6, H6N1, H7N9, H9N2, H10N2, and H11N3) as well as other avian respiratory tract virus strains, including common NDV, IBV, IBDV, APMV-4, MDV, ILTV, and APV. The results showed that the QDFM–ICS only reacts with the H5 subtypes of AIV (including H5N1, H5N2, H5N6, and H5N8) and does not show any cross-reactivity with other subtypes of influenza A viruses or different viruses (Fig. 5). This lack of interference afforded accurate and reliable results for the diagnosis of the intended target virus. Hence, it was evident that the QDFM–ICS exhibits high specificity for detecting H5 AIVs.

Stability of H5 QD-ICS

The QDFM–ICS strips stored at 4 °C and those at room temperature for 3 months demonstrated sustained sensitivity against 0.0625 HA units of the H5 subtype of AIVs, which is equivalent to that of a newly produced strip (Table 5). In comparison, the strips stored at 40 °C for 1 month maintained their sensitivity for detecting H5 AIVs, while prolonged storage for 2 months reduced their sensitivity to 1 HAU, with a further decline after 3 months. Notably, the QDFM–ICS strips maintained their

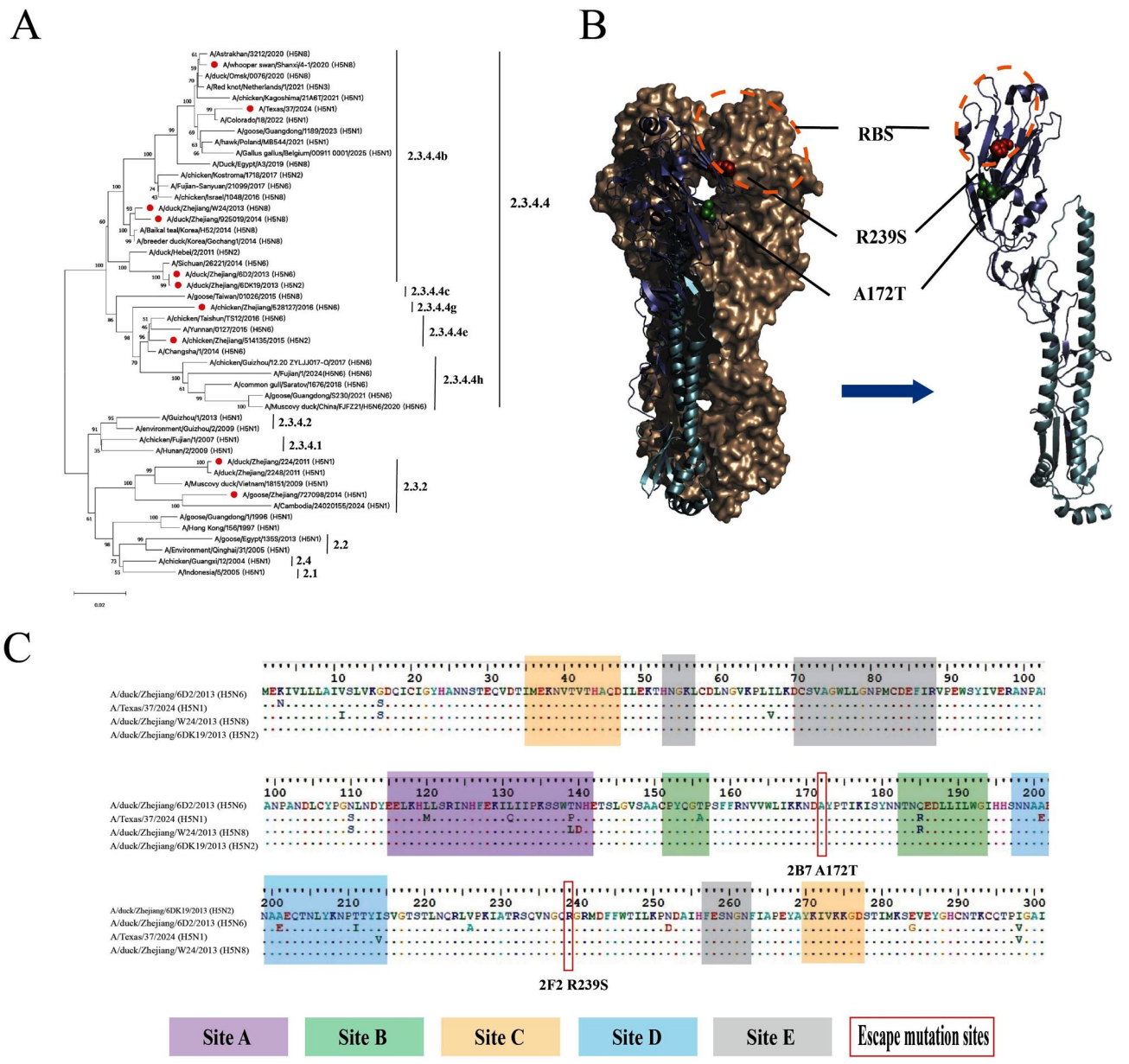

Fig. 3 Phylogenetic and mutation site analyses of H5 AIVs. (**A**) Phylogenetic tree of the HA genes of representative H5 influenza viruses collected from 1996 to 2025 in the GISAID, generated using the Neighbor-Joining method and bootstrapped with 1000 replicates in MEGA 11. The influenza viruses included are highlighted by red dots. (**B**) Escape mutations are shown in the crystal structure of A/Sichuan/26,221/2014 (H5N6) using Pymol based on the RCSB PDB entry 5HU8. Red, mAb 2F2; green, mAb2B7. The mAbs escape mutation regions are indicated by the corresponding color. Orange dashed circle, receptor binding site (RBS) of HA protein (orange). RBS is located in the HA1 head region and contains 190-helix, 130-loop, 150-loop, 220-loop, and other amino acid residues. (**C**) HA gene sequence alignments of H5 virus and escape mutant variants of mAbs 2B7 and 2F2. Five antigenic sites A, B, C, D, and E were inferred by mapping the three-dimensional structure of H5 HA (PDB accession number, 5HU8), labeled in purple, green, orange, blue, and gray. The escape mutation sites recognized by mAbs 2F2 and 2B7 are depicted in red

specificity for detecting H5 AIVs without any alterations. This observation is supported by the evidence that there were no false positive results under any of the tested storage conditions. Apparently, 3 months of storage at 4 °C and room temperature and 1month at 40 °C do not cause any decline in the performance of the QDFM–ICS method for detecting H5 AIV.

Actual application of H5 QDFM-ICS in vitro sample tests

Among the 160 avian samples (30 throat swabs, 30 cloacal swabs, and 100 fecal samples), 35 were confirmed H5-positive using real-time PCR assay. These 35 samples were used as the reference standard for comparing the real-time PCR assay with the QDFM-ICS method and to evaluate the accuracy of our proposed method. This comparison helped in determining the effectiveness of

Table 3 Polymorphism analysis of amino acid residues

Mab	Residue	Percentage of amino acid mutation sites in the H5 subtype of AIVs epidemic strain (%)					
		-2005	2005–2010	2011–2019	2020–2022	2023–2025	Total
		(*n* = 704)	(*n* = 3091)	(*n* = 8246)	(*n* = 12965)	(*n* = 8857)	(*n* = 33863)
2B7	A172T	A 172 (402, 57.1%);	A 172 (3022, 97.78%);	A 172 (7255, 87.98%);	A 172 (12786, 98.62%);	A 172 (8630, 97.44%);	A 172 (32095, 94.78%);
		T 172 (202, 28.7%)	T 172 (28, 0.91%)	T 172 (685, 8.31%)	T 172 (103, 0.80%)	T 172 (180, 2.03%)	T 172 (1198, 3.53%)
		Others (100, 14.2%)	Others (41, 1.32%)	Others (306, 3.71%)	Others (76, 0.58%)	Others (47, 0.53%)	Others (570, 1.69%)
2F2	R239S	R 239 (702, 99.7%);	R 239 (3085, 99.81%);	R 239 (3649, 44.26%);	R 239 (12613, 97.29%);	R 239 (8521, 96.21%);	R 239 (28570, 84.31%);
		S 239 (2, 0.03%)	S 239 (0, 0.00%)	S 239 (4006, 48.59%)	S 239 (339, 2.62%)	S 239 (319, 3.61%)	S 239 (4666, 13.78%)
		Others (0, 0.00%)	Others (6, 0.19%)	Others (591, 7.15%)	Others (13, 0.09%)	Others (17, 0.18%)	Others (627, 0.05%)

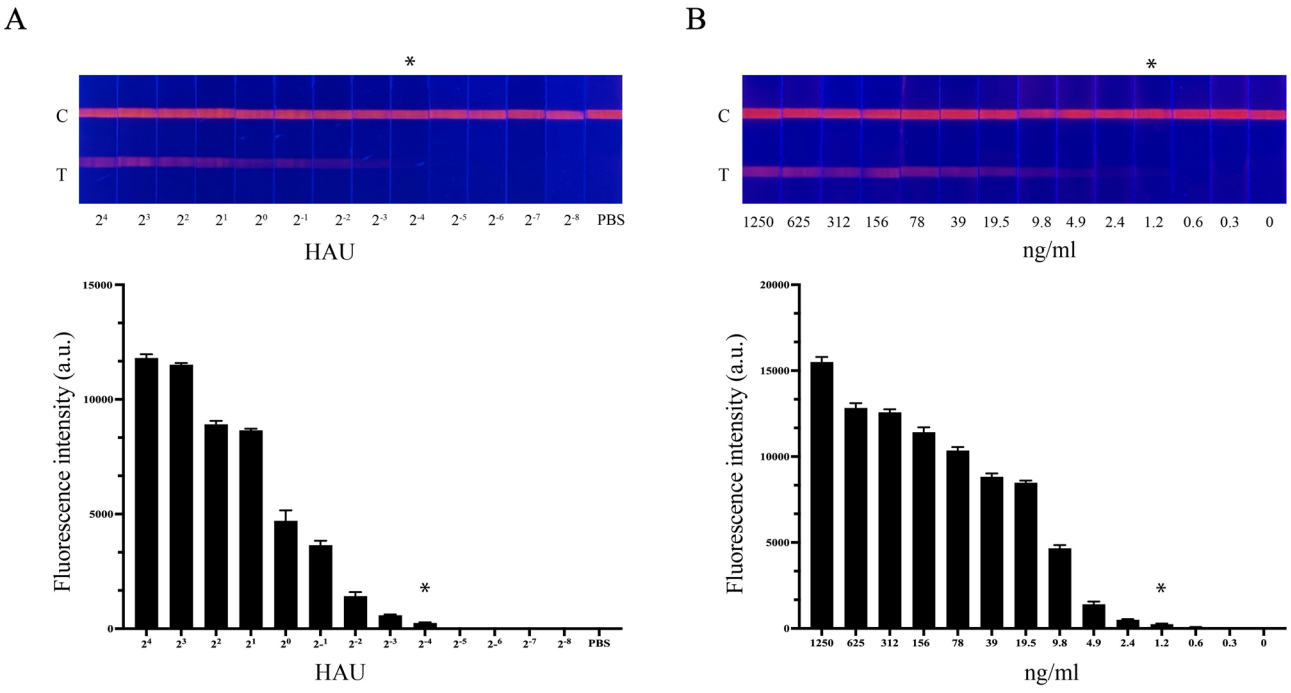

Fig. 4 Images of tested H5 QDFM-CIS in response to the excitation of 365-nm ultraviolet light. Fluorescence viewed by naked eyes. The asterisk indicated the LOD of the strips, which could reach up to 2^{-4} HAU (A) and 1.2 ng/mL purified H5N6 HA protein (B), as determined from the H5 antigen test line. Fluorescence intensity detected by the fluorescence test strip scanner. The asterisk indicates the LOD value

Table 4 Repeatabilityof H5 QDFM-ICS

Viral concentration (HAU)	Mean	Standard deviation	CV%
2^4	11,801	170.5	1.4%
2^3	11,512	70.8	0.6%
2^2	8914	151.8	1.7%
2^1	8647	68.8	0.8%
2^0	4705	455.8	9.7%
$2-^1$	3642	195.4	5.4%
2^{-2}	1449	138.2	9.5%
2^{-3}	584	33.9	5.8%
2^{-4}	253	23.2	9.1%

Mean values refer to the average fluorescence intensity(a.u.) (*n* = 20)

Standard deviation (Std. Dev.) values refer to the the standard deviation of fluorescence (*n* = 20)

CV% refers to the coefficient of variation, calculated as (Std. Dev./Mean × 100)

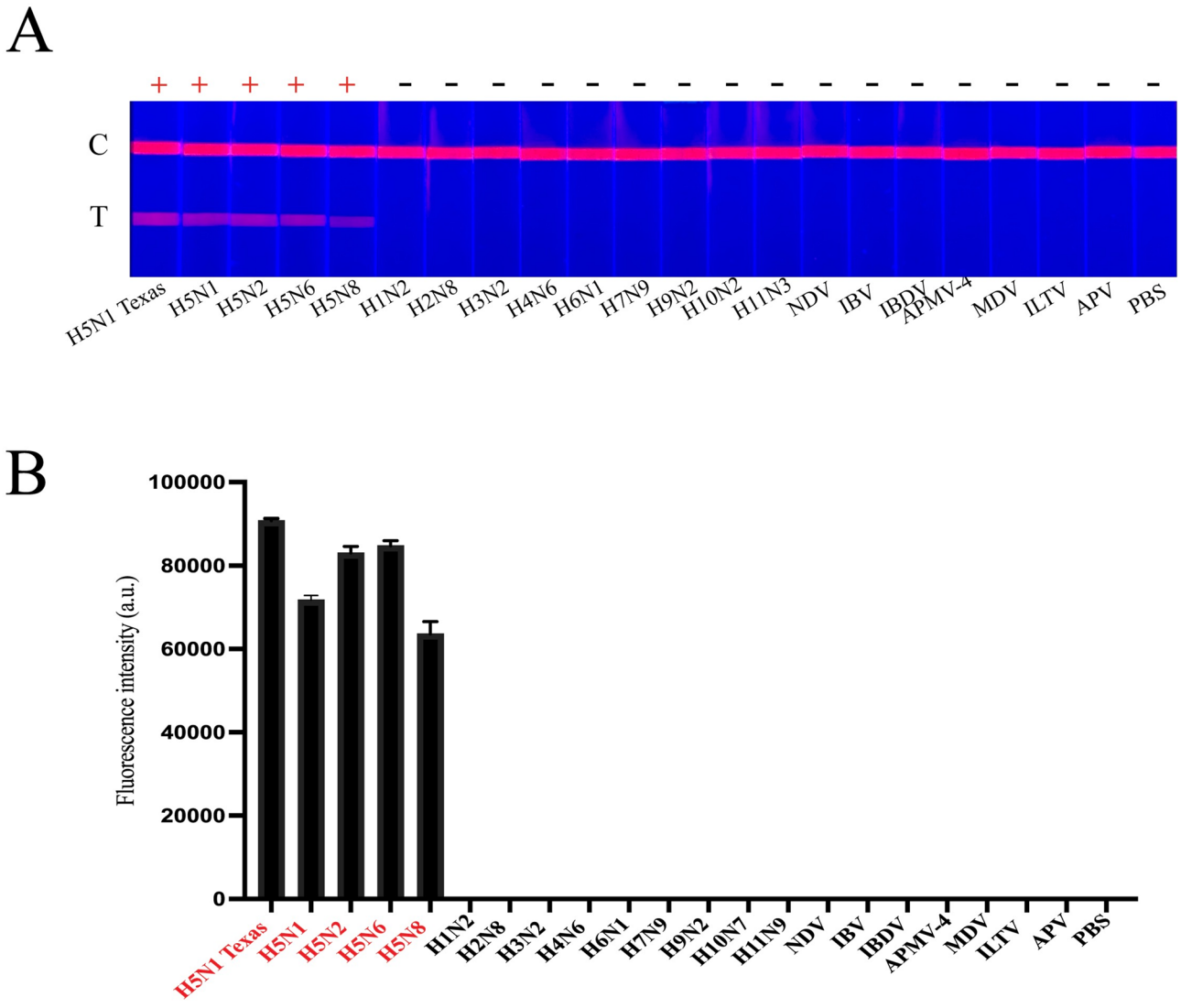

Fig. 5 Cross-reactivity detection of tested H5 QDFM-CIS in response to influenza A and other avian viruses. (**A**) Fluorescence viewed by naked eyes demonstrates that the strips specifically bound to the H5 subtype of influenza virus without cross-reactivity with other influenza A virus subtypes (including H5N1, H5N2, H5N6, H5N8, H1N2, H2N8, H3N2, H4N6, H5N6, H6N1, H7N9, H9N2, H10N2, and H11N3) or other avian viruses (including NDV, IBV, IBDV, APMV-4, MDV, ILTV, and APV). (**B**) Fluorescence intensity detected by the fluorescence test-strip scanner

Table 5 Stability of H5 QDFM-ICS

Storage period	Temperature	LOD of H5 QDs-ICS (HAU)	Positive results	Negative results
1 month	4 °C	2^{-4}	20	10
	Room temperature	2^{-4}	20	10
	40 °C	2^{-4}	20	10
2 months	4 °C	2^{-4}	20	10
	Room temperature	2^{-4}	20	10
	40 °C	2^{-2}	20	10
3 months	4 °C	2^{-4}	20	10
	Room temperature	2^{-4}	20	10
	40 °C	2^{0}	20	10

Table 6 Sample testing using QDFM-ICS and real-time PCR

Sample origin	QDFM-ICS result		Real-time PCR result		Total
	Positive	Negative	Positive	Negative	
Throat swab	5	25	5	25	30
Cloacal swab	8	22	8	22	30
Fecal samples	22	78	22	78	100

Real-time PCR was served as the gold standard to evaluate the accuracy of the established method

the QDFM-ICS method in comparison to the established real-time PCR technique. As described in Table 6, both methods yielded identical results, indicating a perfect 100% agreement. Hence, it can be suggested that the QDFM-ICS exhibited reliable performance across different sample types, while maintaining high sensitivity and specificity.

Discussion

H5 subtype AIVs have evolved mainly through genome mutations, accumulations, and recombinations with different virus strains. The unprecedented mutations and reassortment of the internal gene segments of these viruses have enabled them to breach the species barrier and transmit to ever newer mammalian species, such as seals, seabirds, foxes, and even humans. It also explains the worldwide sweep of Asian-origin H5 HPAI viruses [40]. H5 AIV-caused human infections have been periodically reported since the 20th century. Some of these infections even resulted in deaths, especially those caused by the H5 HPAI virus strain. From 2014 to 2022, 87 cases of H5N6 infection were reported in humans [40]. Russia confirmed the first case of human infection of H5N8 in 2020 [41]. In December 2024, the CDC confirmed the first severe case [42, 43]. Because the H5 HPAI subtype causes severe respiratory infections that may even turn fatal, it is essential to urgently develop a rapid and sensitive detection method for these viruses.

Timely and precise detection is crucial for monitoring the spread of these viruses and implementing appropriate measures to control and prevent their outbreaks. The current mainstream detection techniques are based on the antigen–antibody reactions, such as ELISA and the colloidal gold-based immunochromatographic test (ICT) strip. In these methods, antigen capture and detection are conducted through two mAbs presented at different sites of the same antigen [44]. Both ELISA and ICT allow precise and rapid identification of influenza viruses. Multiple studies have investigated the generation and detection methods for mAbs of the influenza virus. For example, Paparoditis et al. developed the blocking of binding ELISA method to detect potent heterosubtypic antibodies targeting the HA stem region of the influenza virus, especially human mAbs [45]. Researchers also designed a colloidal gold-based ICT strip for instant testing AIV using two mAbs, with a detection limit of 2 HAU [46]. However, it is necessary to optimize the LODs of these methods. QD-labeled mAbs may enable sensitive, instant, and economical detection of various viruses, including the influenza virus. Wu et al. established a rapid and quantitative detection method for the H7N9 virus by employing simultaneous magnetic capture and QD labeling, which allowed clinical recognition and confirmation of H7N9-infected cases [47]. A previous study reported a QD-based fluorescent immunochromatographic assay specifically for detecting SARS-CoV-2. This advanced method can identify the virus in only 15 min, with an impressive detection limit (5 pg/mL) for the virus antigen [38]. It has already been used for detecting the Zika virus. Adegoke et al. constructed a plasmonic nanoparticle–QD hybrid with a detection limit of < 3 copies/mL [48].

This study discusses the development of a QDFM-ICS method, based on suitable mAbs, for rapid and sensitive detection of H5 subtype AIV. The mAbs separated through a hybridoma technique revealed strong binding affinities, specificities, and neutralization potency with the H5 subtype virus with an HI titter of 1 mg/ml (2B7) and 7 mg/ml (2F2) respectively, while the both MN abilities could reach to 0.78 ug/mL. Furthermore, we identified the escape mutation sites of two mAbs as 2F2 R239S and 2B7 A172T. Mutation 239 is located in the receptor-binding region, while mutation 172 is a potential glycosylation site. In general, the avian-type receptor is α-2, 3-linked sialic acid, whereas the human-type receptor is α-2, 6-linked sialic acid. Previous studies have shown that H5 HA requires receptor-binding site (RBS) mutations to switch the receptor specificity from α-2,3-linked sialic acid to α-2,6-linked sialic acid, which makes the virus a pandemic threat [49–51]. Enveloped viruses typically tend to accumulate *N*-glycosylation sites as a common immune evasion strategy. Glycans on influenza hemagglutinin impact the receptor binding and immune response. Their modification is critical for the AIV life cycle [52, 53], which might be a possible mechanism through which mAbs affect the virus. The sustained high conservation at both mutation sites reinforces the view that the selected mAbs can be used in various clinical applications and for producing antiviral drugs and vaccines. Besides, timely monitoring any change in the consistency of the virus antigen and building the mutation database may help in handling any possible future HPAI H5 outbreaks, as it will significantly compress the

response time. Our QDFM-ICS method is based on these specific mAbs and has a sensitive LOD of 0.0625 HAU of H5 AIVs H5, including those of the current circulating strain. The high specificity shows that it can accurately identify the H5 virus, which helps reduce chances of missed and false negative diagnosis. Meanwhile, the good reproducibility enabled the reliability of the whole detection system. Compared to traditional detection approaches, such as ELISA and colloidal gold-based immunochromatographic assays that require tedious processing steps, our QDFM-ICS has a more convenient detection approach, is rapid (can be completed within 15 min), and has a simpler operation. Furthermore, the measurement methodology used in our method could be used to establish other virus-detection methods by replacing the oriented antibody pairs. Hence, it can be suggested that our QDFM-ICS method has a strong application value.

Conclusion

This study developed a rapid, sensitive, and specific QDFM-ICS using two mAbs (2F2 and 2B7) for detecting the H5 subtype influenza virus. The detection limit was 0.0625 HAU per 80 μL of live H5 AIVs and 1.2 ng/mL purified H5N6 HA protein. This method allows rapid discrimination of results (within 15 min). Importantly, the results can be stably reproduced as well. Moreover, clinical sample testing showed excellent consistency between the QDFM-ICS and real-time PCR results. These results suggest that mAb-based QDFM-ICS can be a promising tool for rapid detection of H5 subtype AIVs and may prove useful in any future HPAI H5 pandemics.

Abbreviations

AIVs	Avian influenza viruses
QDFM-ICS	Quantum dot fluorescent microsphere-based immunochromatographic strip
QDs	Quantum dots
HA	Haemagglutinin
NA	Neuraminidase
HPAI	Highly pathogenic avian influenza
OIE-WAHIS	The World Animal Health Information System
WHO	The World Health Organization
ELISA	Enzyme-linked immunoassays assay
RT-PCR	Real-time reverse transcriptase PCR
POCT	Point-of-care testing
LOD	The limit of detection
PBS	Phosphate-buffered saline
IFA	Immunofluorescence assay
MOI	Multiplicity of infection
BSA	Bovine serum albumin
HAI	Hemagglutination inhibition
HAU	HA units
MN	Microneutralization
TCID50	50% tissue culture infectious doses
CPE	Cytopathic effect
IC_{50}	Inhibit virus replication by 50%
MES	4-morpholineethanesulfonic acid
EDC	1-ethyl-3-(3-dimethylaminopropyl) carbodiimide hydrochloride
NHS	N-hydroxysuccinimide
PVC	Polyvinyl chloride
NC	Nitrocellulose
APMV-4	Avian paramyxovirus-4
IBV	Infectiousbronchitisvirus
IBDV	Infectiousbursaldiseasevirus
MDV	Marek'sdisease vírus
ILTV	Infectiouslaryngotracheitis vírus
APV	Avianpox vírus
NDV	Newcastle diseasevirus
CV	Coefficient of variation
MARMs	Monoclonal antibodyresistantmutants
RBD	Receptor-binding domain
RBS	Receptor-binding site
ICT	Immunochromatographic test

Author contributions

HW, PW and JF conducted the experiments, analyzed the data, and wrote the manuscript. FY, LC, FL, HY, NW and LX participated in the data analysis and manuscript writing. HW and LL reviewed and revised the manuscript. All the authors have read and approved the final version of manuscript.

Funding

This study was supported by Grants from the National Science Foundation of the People's Republic of China (No.32273092), Zhejiang Provincial Natural Science Foundation of China (No.LY24H190001), the Fundamental Research Funds for the Central Universities (No.2022ZFJH003) and National Key R&D Program of China (No.2024YFC2309903).

Data availability

No datasets were generated or analysed during the current study.

Declarations

Ethics approval and consent to participate

All animal experiments were conducted in accordance with the Animal Ethics Procedures and Guidelines of the People's Republic of China. The study protocol was approved by the Animal Ethics Committee of the First Affiliated Hospital, School of Medicine, Zhejiang University (Approval No. 2022-16).

Competing interests

The authors declare no competing interests.

Received: 15 March 2025 / Accepted: 15 July 2025
Published online: 18 July 2025

References

1. Kang M, Wang LF, Sun BW, Wan WB, Ji X, Baele G, Bi YH, Suchard MA, Lai A, Zhang M, et al. Zoonotic infections by avian influenza virus: changing global epidemiology, investigation, and control. Lancet Infect Dis. 2024;24:e522–31.
2. Jimenez-Bluhm P, Siegers JY, Tan S, Sharp B, Freiden P, Johow M, Orozco K, Ruiz S, Baumberger C, Galdames P, et al. Detection and phylogenetic analysis of highly pathogenic A/H5N1 avian influenza clade 2.3.4.4b virus in chile, 2022. Emerg Microbes Infect. 2023;12:2220569.
3. Lu M, He WT, Pettersson JH, Baele G, Shi M, Holmes EC, He N, Su S. Zoonotic risk assessment among farmed mammals. *Cell*. 2023, 186:2040–2040.e2041.
4. Eisfeld AJ, Biswas A, Guan L, Gu C, Maemura T, Trifkovic S, Wang T, Babujee L, Dahn R, Halfmann PJ, et al. Pathogenicity and transmissibility of bovine H5N1 influenza virus. Nature. 2024;633:426–32.
5. Uyeki TM. Global epidemiology of human infections with highly pathogenic avian influenza A (H5N1) viruses. Respirology. 2008;13(Suppl 1):S2–9.
6. Krammer F, Schultz-Cherry S. We need to keep an eye on avian influenza. Nat Rev Immunol. 2023;23:267–8.
7. Antigua KJC, Choi WS, Baek YH, Song MS. The emergence and decennary distribution of clade 2.3.4.4 HPAI H5Nx. Microorganisms 2019, 7.
8. Hassan KE, King J, El-Kady M, Afifi M, Abozeid HH, Pohlmann A, Beer M, Harder T. Novel reassortant highly pathogenic avian influenza A(H5N2) virus in broiler chickens, Egypt. Emerg Infect Dis. 2020;26:129–33.
9. HIGH PATHOGENICITY AVIAN INFLUENZA (HPAI). Situation Report 66 [https://www.woah.org/en/document/high-pathogenicity-avian-influenza-hpai-situation-report-66/]

10. Cumulative number of confirmed human cases for avian influenza A(H5N1) reported to WHO. 2003–2025 [https://cdn.who.int/media/docs/default-source/2021-dha-docs/cumulative-number-of-confirmed-human-cases-for-avian-influenza-a(h5n1)-reported-to-who--2003-2025.pdf?sfvrsn=e1871d4c_5&download=true]
11. Li KS, Guan Y, Wang J, Smith GJ, Xu KM, Duan L, Rahardjo AP, Puthavathana P, Buranathai C, Nguyen TD, et al. Genesis of a highly pathogenic and potentially pandemic H5N1 influenza virus in Eastern Asia. Nature. 2004;430:209–13.
12. Shen H, Wu B, Chen Y, Bi Y, Xie Q, Influenza. A(H5N6) virus reassortant, Southern china, 2014. Emerg Infect Dis. 2015;21:1261–2.
13. Bi Y, Tan S, Yang Y, Wong G, Zhao M, Zhang Q, Wang Q, Zhao X, Li L, Yuan J, et al. Clinical and immunological characteristics of human infections with H5N6 avian influenza virus. Clin Infect Dis. 2019;68:1100–9.
14. Lee YJ, Kang HM, Lee EK, Song BM, Jeong J, Kwon YK, Kim HR, Lee KJ, Hong MS, Jang I, et al. Novel reassortant influenza A(H5N8) viruses, South korea, 2014. Emerg Infect Dis. 2014;20:1087–9.
15. Rafique S, Rashid F, Mushtaq S, Ali A, Li M, Luo S, Xie L, Xie Z. Global review of the H5N8 avian influenza virus subtype. Front Microbiol. 2023;14:1200681.
16. Technical report. June 2024 Highly pathogenic avian influenza A(H5N1) viruses [https://www.cdc.gov/bird-flu/php/technical-report/h5n1-06052024.html.].
17. Uyeki TM, Milton S, Abdul Hamid C, Reinoso Webb C, Presley SM, Shetty V, Rollo SN, Martinez DL, Rai S, Gonzales ER, et al. Highly pathogenic avian influenza A(H5N1) virus infection in a dairy farm worker. N Engl J Med. 2024;390:2028–9.
18. Caserta LC, Frye EA, Butt SL, Laverack M, Nooruzzaman M, Covaleda LM, Thompson AC, Koscielny MP, Cronk B, Johnson A, et al. Spillover of highly pathogenic avian influenza H5N1 virus to dairy cattle. Nature. 2024;634:669–76.
19. Peacock T, Moncla L, Dudas G, VanInsberghe D, Sukhova K, Lloyd-Smith JO, Worobey M, Lowen AC, Nelson MI. The global H5N1 influenza panzootic in mammals. Nature 2024.
20. Jahangir MA, Gilani SJ, Muheem A, Jafar M, Aslam M, Ansari MT, Barkat MA. Quantum dots: next generation of smart Nano-Systems. Pharm Nanotechnol. 2019;7:234–45.
21. Bian F, Sun L, Cai L, Wang Y, Zhao Y. Quantum Dots from microfluidics for nanomedical application. Wiley Interdiscip Rev Nanomed Nanobiotechnol. 2019;11:e1567.
22. Li C, Zou Z, Liu H, Jin Y, Li G, Yuan C, Xiao Z, Jin M. Synthesis of polystyrene-based fluorescent quantum Dots nanolabel and its performance in H5N1 virus and SARS-CoV-2 antibody sensing. Talanta. 2021;225:122064.
23. Li J, Liu B, Tang X, Wu Z, Lu J, Liang C, Hou S, Zhang L, Li T, Zhao W, et al. Development of a smartphone-based quantum Dot lateral flow immunoassay strip for ultrasensitive detection of anti-SARS-CoV-2 IgG and neutralizing antibodies. Int J Infect Dis. 2022;121:58–65.
24. Yin W, Li W, Li Q, Qin C, Zhang Z, Zhang X, Zhang XE, Cui Z. Structural characterization and analysis of human immunodeficiency virus encapsulating quantum Dots. J Nanosci Nanotechnol. 2018;18:4487–94.
25. Pijeira MSO, de Menezes AS, Fechine PBA, Shah SQ, Ilem-Ozdemir D, López EO, Maricato JT, Rosa DS, Ricci-Junior E, Junior SA, et al. Folic acid-functionalized graphene quantum dots: synthesis, characterization, radiolabeling with radium-223 and antiviral effect against Zika virus infection. Eur J Pharm Biopharm. 2022;180:91–100.
26. He Q, Velumani S, Du Q, Lim CW, Ng FK, Donis R, Kwang J. Detection of H5 avian influenza viruses by antigen-capture enzyme-linked immunosorbent assay using H5-specific monoclonal antibody. Clin Vaccine Immunol. 2007;14:617–23.
27. Gupta N, Augustine S, Narayan T, O'Riordan A, Das A, Kumar D, Luong JHT, Malhotra BD. Point-of-Care PCR assays for COVID-19 detection. Biosens (Basel). 2021, 11.
28. Bruchez M Jr., Moronne M, Gin P, Weiss S, Alivisatos AP. Semiconductor nanocrystals as fluorescent biological labels. Science. 1998;281:2013–6.
29. Hahn MA, Keng PC, Krauss TD. Flow cytometric analysis to detect pathogens in bacterial cell mixtures using semiconductor quantum Dots. Anal Chem. 2008;80:864–72.
30. Wu H, Lu R, Peng X, Xu L, Cheng L, Lu X, Jin C, Xie T, Yao H, Wu N. Novel reassortant highly pathogenic H5N6 avian influenza viruses in poultry in China. Infect Genet Evol. 2015;31:64–7.
31. Yang F, Xiao Y, Lu R, Chen B, Liu F, Wang L, Yao H, Wu N, Wu H. Generation of neutralizing and non-neutralizing monoclonal antibodies against H7N9 influenza virus. Emerg Microbes Infect. 2020;9:664–75.
32. Tan Y, Ng Q, Jia Q, Kwang J, He F. A novel humanized antibody neutralizes H5N1 influenza virus via two different mechanisms. J Virol. 2015;89:3712–22.
33. Nogales A, Piepenbrink MS, Wang J, Ortega S, Basu M, Fucile CF, Treanor JJ, Rosenberg AF, Zand MS, Keefer MC, et al. A highly potent and broadly neutralizing H1 Influenza-Specific human monoclonal antibody. Sci Rep. 2018;8:4374.
34. Wu WL, Chen Y, Wang P, Song W, Lau SY, Rayner JM, Smith GJ, Webster RG, Peiris JS, Lin T, et al. Antigenic profile of avian H5N1 viruses in Asia from 2002 to 2007. J Virol. 2008;82:1798–807.
35. Ito M, Yamayoshi S, Murakami K, Saito K, Motojima A, Nakaishi K, Kawaoka Y. Characterization of mouse monoclonal antibodies against the HA of A(H7N9) influenza virus. Viruses 2019, 11.
36. Wu F, Yuan H, Zhou C, Mao M, Liu Q, Shen H, Cen Y, Qin Z, Ma L, Song Li L. Multiplexed detection of influenza A virus subtype H5 and H9 via quantum dot-based immunoassay. Biosens Bioelectron. 2016;77:464–70.
37. Nguyen AVT, Dao TD, Trinh TTT, Choi DY, Yu ST, Park H, Yeo SJ. Sensitive detection of influenza a virus based on a cdse/cds/zns quantum dot-linked rapid fluorescent immunochromatographic test. Biosens Bioelectron. 2020;155:112090.
38. Wang C, Yang X, Zheng S, Cheng X, Xiao R, Li Q, Wang W, Liu X, Wang S. Development of an ultrasensitive fluorescent immunochromatographic assay based on multilayer quantum Dot nanobead for simultaneous detection of SARS-CoV-2 antigen and influenza A virus. Sens Actuators B Chem. 2021;345:130372.
39. Peng F, Wang Z, Zhang S, Wu R, Hu S, Li Z, Wang X, Bi D. Development of an immunochromatographic strip for rapid detection of H9 subtype avian influenza viruses. Clin Vaccine Immunol. 2008;15:569–74.
40. Huang P, Sun L, Li J, Wu Q, Rezaei N, Jiang S, Pan C. Potential cross-species transmission of highly pathogenic avian influenza H5 subtype (HPAI H5) viruses to humans calls for the development of H5-specific and universal influenza vaccines. Cell Discov. 2023;9:58.
41. Shi J, Zeng X, Cui P, Yan C, Chen H. Alarming situation of emerging H5 and H7 avian influenza and effective control strategies. Emerg Microbes Infect. 2023;12:2155072.
42. H5 Bird Flu. Curr Situation [https://www.cdc.gov/bird-flu/situation-summary/index.html]
43. CDC Confirms Second. Human H5 bird flu case in michigan; third case tied to dairy outbreak. [www.cdc.gov/media/releases/2024/p0530-h5-human-case-michigan.html]
44. Sun Z, Shi B, Meng F, Ma R, Hu Q, Qin T, Chen S, Peng D, Liu X. Development of a Colloidal Gold-Based Immunochromatographic Strip for Rapid Detection of H7N9 Influenza Viruses. *Front Microbiol.* 2018, 9:2069.
45. Paparoditis PCG, Fruehwirth A, Bevc K, Low JS, Jerak J, Terzaghi L, Foglierini M, Fernandez B, Jarrossay D, Corti D, et al. Site-specific serology unveils cross-reactive monoclonal antibodies targeting influenza A hemagglutinin epitopes. Eur J Immunol. 2024;54:e2451045.
46. Yang F, Xiao Y, Chen B, Wang L, Liu F, Yao H, Wu N, Wu H. Development of a colloidal gold-based immunochromatographic strip test using two monoclonal antibodies to detect H7N9 avian influenza virus. Virus Genes. 2020;56:396–400.
47. Wu M, Zhang ZL, Chen G, Wen CY, Wu LL, Hu J, Xiong CC, Chen JJ, Pang DW. Rapid and quantitative detection of avian influenza A(H7N9) virions in complex matrices based on combined magnetic capture and quantum Dot labeling. Small. 2015;11:5280–8.
48. Adegoke O, Morita M, Kato T, Ito M, Suzuki T, Park EY. Localized surface plasmon resonance-mediated fluorescence signals in plasmonic nanoparticle-quantum Dot hybrids for ultrasensitive Zika virus RNA detection via hairpin hybridization assays. Biosens Bioelectron. 2017;94:513–22.
49. Herfst S, Schrauwen EJ, Linster M, Chutinimitkul S, de Wit E, Munster VJ, Sorrell EM, Bestebroer TM, Burke DF, Smith DJ, et al. Airborne transmission of influenza A/H5N1 virus between ferrets. Science. 2012;336:1534–41.
50. Imai M, Watanabe T, Hatta M, Das SC, Ozawa M, Shinya K, Zhong G, Hanson A, Katsura H, Watanabe S, et al. Experimental adaptation of an influenza H5 HA confers respiratory droplet transmission to a reassortant H5 HA/H1N1 virus in ferrets. Nature. 2012;486:420–8.
51. de Vries RP, Zhu X, McBride R, Rigter A, Hanson A, Zhong G, Hatta M, Xu R, Yu W, Kawaoka Y, et al. Hemagglutinin receptor specificity and structural analyses of respiratory droplet-transmissible H5N1 viruses. J Virol. 2014;88:768–73.
52. Medina RA, García-Sastre A, Influenza. A viruses: new research developments. Nat Rev Microbiol. 2011;9:590–603.

53. Wang CC, Chen JR, Tseng YC, Hsu CH, Hung YF, Chen SW, Chen CM, Khoo KH, Cheng TJ, Cheng YS, et al. Glycans on influenza hemagglutinin affect receptor binding and immune response. Proc Natl Acad Sci U S A. 2009;106:18137–42.

Publisher's note